

Scotogenic generation of realistic neutrino mixing with D5

Soumita Pramanick^{1*}

¹ *Physical Research Laboratory, Ahmedabad, Gujarat, 380009, India*

Abstract

A mechanism of radiative generation of realistic neutrino mixing at one-loop level with $D5 \times Z_2$ is presented in this paper. The process is demonstrated in two set-ups using $D5 \times Z_2$ symmetry viz. Model 1 and Model 2. Two right-handed neutrinos are present in both the models. In both Model 1 and Model 2, when mixing between these two right-handed neutrinos are maximal, one can produce the form of the left-handed Majorana neutrino mass matrix corresponding to $\theta_{13} = 0$, $\theta_{23} = \pi/4$ and any value of θ_{12}^0 associated with Tribimaximal (TBM), Bimaximal (BM), Golden Ratio (GR) or other mixings. Small shift from maximal mixing between the two right-handed neutrino states can generate non-zero θ_{13} , deviation of θ_{23} from $\pi/4$ and corrections to the solar mixing θ_{12} in one step for both Model 1 and Model 2. In both the models, two Z_2 odd inert $SU(2)_L$ doublet scalars are present. The lightest between these two scalars can be a viable dark matter candidate for both Model 1 and Model 2.

I Introduction

Neutrinos oscillate as they are massive. The Pontecorvo, Maki, Nakagawa, Sakata – PMNS – matrix connecting the neutrino mass eigenstates with its flavour eigenstates is given by:

$$U = \begin{pmatrix} c_{12}c_{13} & s_{12}c_{13} & -s_{13}e^{-i\delta} \\ -c_{23}s_{12} + s_{23}s_{13}c_{12}e^{i\delta} & c_{23}c_{12} + s_{23}s_{13}s_{12}e^{i\delta} & -s_{23}c_{13} \\ -s_{23}s_{12} - c_{23}s_{13}c_{12}e^{i\delta} & s_{23}c_{12} - c_{23}s_{13}s_{12}e^{i\delta} & c_{23}c_{13} \end{pmatrix}. \quad (1)$$

The c_{ij} and s_{ij} in Eq. (1) denote $\cos \theta_{ij}$ and $\sin \theta_{ij}$ respectively. It is noteworthy that the neutrino mass eigenstates are non-degenerate.

The observation of non-zero θ_{13} by short-baseline reactor anti-neutrino experiments [1] in 2012 led to important consequences. It must also be noted that although θ_{13} is non-zero, the value of θ_{13} is small compared to the other two mixing angles. Before the discovery of non-zero θ_{13} , models with leptonic mixings characterized by $\theta_{13} = 0$, $\theta_{23} = \pi/4$ such as Tribimaximal (TBM), Bimaximal (BM), Golden Ratio (GR) mixings (now onwards in this paper we will refer to these mixings collectively as popular lepton mixings) were extensively studied. In order to construct TBM, BM and GR mixing patterns one has to vary θ_{12}^0 to the particular values mentioned in Table (1) keeping $\theta_{13} = 0$ and $\theta_{23} = \pi/4$ fixed. Thus, a common structure for all the popular lepton mixings can be easily obtained by putting $\theta_{13} = 0$ and $\theta_{23} = \pi/4$ in Eq. (1):

$$U^0 = \begin{pmatrix} \cos \theta_{12}^0 & \sin \theta_{12}^0 & 0 \\ -\frac{\sin \theta_{12}^0}{\sqrt{2}} & \frac{\cos \theta_{12}^0}{\sqrt{2}} & -\frac{1}{\sqrt{2}} \\ -\frac{\sin \theta_{12}^0}{\sqrt{2}} & \frac{\cos \theta_{12}^0}{\sqrt{2}} & \frac{1}{\sqrt{2}} \end{pmatrix}, \quad (2)$$

*email: soumita509@gmail.com

Model	TBM	BM	GR
θ_{12}^0	35.3°	45.0°	31.7°

Table 1: θ_{12}^0 values of various popular lepton mixings viz. TBM, BM and GR mixings.

with θ_{12}^0 for TBM, BM and GR displayed in Table (1).

The 3σ global fit [2, 3, 4] of the three neutrino mixing angles viz. θ_{12} , θ_{13} and θ_{23} as per NuFIT5.2 of 2022 [2]:

$$\begin{aligned}
\theta_{12} &= (31.31 - 35.74)^\circ, \\
\theta_{23} &= (39.6 - 51.9)^\circ, \\
\theta_{13} &= (8.19 - 8.89)^\circ.
\end{aligned} \tag{3}$$

Therefore popular lepton mixings are in sharp disagreement with the non-zero θ_{13} . Extensive model-building activities have been taking place after the observation of non-zero θ_{13} so as to incorporate it in the popular lepton mixing frameworks. In [5], attempts have been made to trace a common origin for the two small quantities viz. non-zero θ_{13} and the solar mass splitting (Δm_{solar}^2). In [6], a two-component neutrino mass matrix scenario was considered where the dominant one was associated with oscillation parameters such as the atmospheric mass splitting (Δm_{atm}^2) and $\theta_{23} = \pi/4$ whereas the other oscillation parameters such as the non-zero θ_{13} , θ_{12} , Δm_{solar}^2 as well as deviation of θ_{23} from $\pi/4$ could be generated perturbatively with the help of smaller see-saw [7] contribution¹. In some studies [9, 10], vanishing θ_{13} was obtained with the help of different symmetries and one could yield non-zero θ_{13} by adding some perturbations to the symmetric structures.

The popular lepton mixings were corrected by devising a two-component Lagrangian mechanism at tree-level with the help of discrete flavour symmetries such as A_4 , S_3 in [11, 12]. The type II see-saw dominant contribution of the Lagrangian corresponding to the popular lepton mixings was corrected by a smaller type I see-saw subdominant contribution in these models. An exactly similar study specific to the no solar mixing (NSM) i.e., $\theta_{12}^0 = 0$ case using A_4 symmetry² can be found in [13]. A study of generating TBM radiatively with A_4 can be found in [14]. Some recent studies of realistic neutrino mixings are present in [15, 16]. For some earlier works on scotogenic models, see [17].

In this paper, radiative generation of realistic neutrino mixing with $D_5 \times Z_2$ symmetry will be presented³. Some earlier works on D_5 symmetry can be found in [18, 19].

The prime intent of this work is to use $D_5 \times Z_2$ symmetry to radiatively⁴ produce:

1. The form of the mixing matrix of popular lepton mixing kind given in Eq. (2) corresponding to $\theta_{13} = 0$, $\theta_{23} = \pi/4$ and θ_{12}^0 of any of the options shown in Table (1).
2. Realistic neutrino mixings i.e., non-zero θ_{13} , deviation of θ_{23} from $\pi/4$ and minute corrections to solar mixing θ_{12} .

¹Similar earlier works can be found in [8].

²Solar splitting was absent in the dominant type II see-saw component thereby allowing us to use degenerate perturbation theory for generation of large solar mixing in [13].

³The discrete symmetry D_5 is briefly discussed in Appendix A.

⁴A detailed analysis of radiative neutrino mass models can be found in [20].

Here the neutrino masses and mixings are generated at one-loop level using $D5 \times Z_2$ symmetry. We try to demonstrate the mechanism in two model set-ups viz. Model 1 and Model 2. The two models vary in the $D5$ quantum number assignments of the fields. Needless to mention, both the models contain same types of fields which only differ in their $D5$ charges and both the models follow the same modulus operandi as discussed below:

In both the models, two right-handed neutrinos are present and when the mixing between these two right-handed neutrino states are maximal (i.e., $\pi/4$), the structure of the leptonic mixing matrix corresponding to the popular lepton mixings characterized by $\theta_{13} = 0$ and $\theta_{23} = \pi/4$ as displayed in Eq. (2) can be generated. We will see in course of our discussion that in both the models, a tiny deviation from maximal mixing in between the two right-handed neutrinos can successfully yield the realistic mixings i.e., non-zero θ_{13} , shifts of the atmospheric mixing angle θ_{23} from $\pi/4$ and slight changes in solar mixing θ_{12} , in a single stroke. The process necessitates two Z_2 odd inert $SU(2)_L$ doublet scalars η_i ($i = 1, 2$), the lightest among which can serve as a dark matter candidate. A similar method was implemented in a scotogenic $S3$ symmetric model [21]. In the scotogenic $A4$ model presented in [22], small mass splitting between two-right handed neutrino states were used instead of tweaking the maximal mixing between the right-handed neutrinos to generate realistic mixings such as non-zero θ_{13} , deviation of θ_{23} from $\pi/4$ and minute modifications of θ_{12} .

In Section II.1 we discuss Model 1 in details, followed by a comprehensive analysis of Model 2 in Section II.2 and finally we conclude with a brief account of our findings in Section III. In Appendix A we discuss about the discrete group $D5$ in general and in Appendix B the scalar potentials of both Model 1 and Model 2 have been scrutinized⁵.

II The $D5 \times Z_2$ Models:

The left-handed Majorana neutrino mass matrix in mass basis is given by $M_{\nu L}^{mass} = \text{diag} (m_1, m_2, m_3)$. The flavour basis form of this $M_{\nu L}^{mass}$ for $\theta_{13} = 0$, $\theta_{23} = \pi/4$ and θ_{12}^0 specific to any of the popular lepton mixing alternatives displayed in Table (1) can be easily obtained by using the common structure of leptonic mixing matrix U^0 given in Eq. (2):

$$M_{\nu L}^{flavour} = U^0 M_{\nu L}^{mass} U^{0T} = \begin{pmatrix} a & c & c \\ c & b & d \\ c & d & b \end{pmatrix}. \quad (4)$$

The a, b, c and d in Eq. (4) are:

$$\begin{aligned} a &= m_1 \cos^2 \theta_{12}^0 + m_2 \sin^2 \theta_{12}^0 \\ b &= \frac{1}{2} (m_1 \sin^2 \theta_{12}^0 + m_2 \cos^2 \theta_{12}^0 + m_3) \\ c &= \frac{1}{2\sqrt{2}} \sin 2\theta_{12}^0 (m_2 - m_1) \\ d &= \frac{1}{2} (m_1 \sin^2 \theta_{12}^0 + m_2 \cos^2 \theta_{12}^0 - m_3). \end{aligned} \quad (5)$$

⁵We will see in Appendix B, that although the $D5$ quantum numbers of the scalars in Model 1 and Model 2 are different eventually the scalar potentials for both Model 1 and Model 2 came out to be the same.

Therefore,

$$\tan 2\theta_{12}^0 = \frac{2\sqrt{2}c}{b+d-a}. \quad (6)$$

For neutrino masses to be non-degenerate and realistic, these quantities a, b, c and d have to be non-zero.

As discussed above, for both the models the first step will be to obtain the structure of $M_{\nu L}^{flavour}$ in Eq. (4) radiatively at one-loop level by appropriately choosing the $D5 \times Z_2$ quantum numbers of the fields in the models. As already mentioned, this will require maximal mixing between the two right-handed neutrino states. Once the form $M_{\nu L}^{flavour}$ in Eq. (4) is achieved, one has to tweak the maximal mixing between these two right-handed neutrinos to get the realistic neutrino mixings. The same procedure will be followed for both Model 1 and Model 2 which differ from each other in terms of $D5$ quantum number assignments of the particles present in the models. Let us now analyze the models one by one.

II.1 Model 1

In Model 1, the three left-handed lepton $SU(2)_L$ doublets $L_{\zeta L} \equiv (\nu_{\zeta} \ \zeta^-)_L^T$ where $\zeta = e, \mu, \tau$ are present. Two of these left-handed lepton $SU(2)_L$ doublets i.e., $L_{\mu L}$ and $L_{\tau L}$ transform as 2_1 under D_5 and the D_5 charge of L_{eL} is 1_1 . In addition to these, two Standard Model (SM) gauge singlet right-handed neutrinos $N_{\alpha R}$, ($\alpha = 1, 2$) are also present in this model that transform as 2_2 under D_5 . The scalar sector comprises of two inert $SU(2)_L$ doublet scalars, $\eta_i \equiv (\eta_i^+, \eta_i^0)^T$, ($i = 1, 2$) transforming as 2_2 of D_5 denoted by η . The other two $SU(2)_L$ doublet scalars i.e., $\Phi_j \equiv (\phi_j^+, \phi_j^0)^T$, ($j = 1, 2$) having D_5 charge 2_2 is designated by Φ . Apart from D_5 , the unbroken Z_2 present in the model plays a crucial role under which all the fields except the right-handed neutrinos and scalar η are even. The ϕ_j being Z_2 even can get vacuum expectation value (vev) after spontaneous symmetry breaking (SSB) whereas η_i being odd under Z_2 cannot get vev. Let v_j denote the vevs of ϕ_j^0 i.e., $\langle \Phi_j \rangle \equiv v_j$, ($j = 1, 2$). The particle content of Model 1 along with their specific quantum numbers are displayed in Table (2). In this model, we are dealing with the neutrino sector only. We are working in a basis in which the charged lepton mass matrix is diagonal and the entire mixing originates from the neutrino sector.

At one-loop level, neutrino mass can be obtained radiatively⁶ from Fig. (1) in Model 1. The relevant part of the $D5 \times Z_2$ conserving scalar potential⁷ that contributes to the left-handed Majorana neutrino mass matrix via the four-point scalar vertex in Fig. (1):

$$\begin{aligned} V_{relevant} \supset & \lambda_1 \left[\left\{ (\eta_2^\dagger \phi_2 + \eta_1^\dagger \phi_1)^2 \right\} + h.c. \right] + \lambda_2 \left[\left\{ (\eta_2^\dagger \phi_2 - \eta_1^\dagger \phi_1)^2 \right\} + h.c. \right] \\ & + \lambda_3 \left[\left\{ (\eta_1^\dagger \phi_2)(\eta_2^\dagger \phi_1) + (\eta_2^\dagger \phi_1)(\eta_1^\dagger \phi_2) \right\} + h.c. \right]. \end{aligned} \quad (7)$$

We take all the quartic couplings λ_j ($j = 1, 2, 3$) to be real.

All symmetries under consideration are conserved at all the three vertices of Fig. (1). The $D5 \times Z_2$ conserving Dirac vertices are given by:

$$\mathcal{L}_{Yukawa}|_{(\text{Model 1})} = y_1 [(\bar{N}_{2R}\eta_2^0 + \bar{N}_{1R}\eta_1^0)\nu_e] + y_2 [(\bar{N}_{1R}\eta_2^0)\nu_\tau + (\bar{N}_{2R}\eta_1^0)\nu_\mu] + h.c. \quad (8)$$

⁶Later on in Section (II.2) we will find that the same diagram in Fig. (1) can generate neutrino mass radiatively at one-loop for Model 2 as well. Thus Fig. (1) serves the purpose of neutrino mass generation radiatively at one-loop for both Model 1 and Model 2.

⁷At the four-point scalar vertex in Fig. (1), two η are created and two ϕ are annihilated. Thus only the terms of the scalar potential of $(\eta^\dagger \phi)(\eta^\dagger \phi)$ kind contribute to the left-handed Majorana neutrino mass matrix. The complete scalar potential for both Model 1 and Model 2 are same and can be found in Appendix B.

Leptons	$SU(2)_L$	$D5$	Z_2
$L_{eL} \equiv (\nu_e \ e^-)_L$	2	1_1	1
$L_{\zeta L} \equiv \begin{pmatrix} \nu_\mu & \mu^- \\ \nu_\tau & \tau^- \end{pmatrix}_L$	2	2_1	1
$N_{\alpha R} \equiv \begin{pmatrix} N_{1R} \\ N_{2R} \end{pmatrix}$	1	2_2	-1
Scalars	$SU(2)_L$	$D5$	Z_2
$\Phi \equiv \begin{pmatrix} \phi_1^+ & \phi_1^0 \\ \phi_2^+ & \phi_2^0 \end{pmatrix}$	2	2_2	1
$\eta \equiv \begin{pmatrix} \eta_1^+ & \eta_1^0 \\ \eta_2^+ & \eta_2^0 \end{pmatrix}$	2	2_2	-1

Table 2: Fields in Model 1 with their corresponding quantum numbers. Here we restrict ourselves to the neutrino sector only.

It is imperative to note that owing to the difference in the D_5 quantum numbers of the left-handed neutrinos as displayed in Table (2), the Yukawa couplings of ν_ζ for ($\zeta = \mu, \tau$) transforming as 2_1 of D_5 is different from that of ν_e with D_5 quantum number 1_1 in Eq. (8). Precisely, the Yukawa couplings of ν_ζ for ($\zeta = \mu, \tau$) and ν_e are denoted by y_2 and y_1 respectively.

In the right-handed neutrino sector we have two right-handed neutrinos, N_{1R} and N_{2R} transforming as 2_2 under D_5 . The $D_5 \times Z_2$ invariant direct mass term for the right-handed neutrinos:

$$\mathcal{L}_{right\text{-handed neutrinos}} = \frac{1}{2} m_{R12} [N_{1R}^T C^{-1} N_{2R} + N_{2R}^T C^{-1} N_{1R}]. \quad (9)$$

Therefore, in a D_5 conserving scenario only non-zero off-diagonal entries are allowed in the right-handed Majorana neutrino mass matrix. To get non-zero diagonal entries, one can add soft D_5 breaking terms:

$$\mathcal{L}_{soft} = \frac{1}{2} [m_{R11} N_{1R}^T C^{-1} N_{1R} + m_{R22} N_{2R}^T C^{-1} N_{2R}] \quad (10)$$

This enables us to write the right-handed neutrino mass matrix as the following:

$$M_{\nu_R} = \frac{1}{2} \begin{pmatrix} m_{R11} & m_{R12} \\ m_{R12} & m_{R22} \end{pmatrix}. \quad (11)$$

This symmetric form of the right-handed neutrino mass matrix⁸ is indicative of its Majorana nature.

⁸We will see later on in Section (II.2), that although the D_5 charges of the right-handed neutrinos in Model 1 differ from that in Model 2, one can still arrive to this form of the right-handed Majorana neutrino mass matrix shown in Eq. (11) in Model 2 as well.

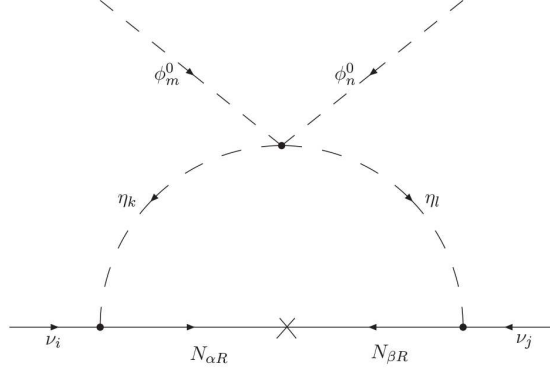


Figure 1: Scotogenic neutrino mass generation at one-loop level with $D5 \times Z_2$ symmetry. This figure is responsible for neutrino mass generation in both Model 1 and Model 2.

At this stage it is prudent to have a look at the dark matter candidates present in the model. It is a general practice to appoint Z_2 symmetry to stabilize the dark matter candidates in the model and since this model also has a Z_2 symmetry, one can immediately perceive the existence of dark matter candidates in the model. From Table (2), we can see that both the right-handed neutrinos $N_{\alpha R}$ with ($\alpha = 1, 2$) as well as the scalars η are odd under Z_2 . Here, we choose η to be lighter than the right-handed neutrinos $N_{\alpha R}$, ($\alpha = 1, 2$). From m_η^2 term in Eq. (B.1) it might seem that the η_i , ($i = 1, 2$) scalars are degenerate in mass, but since $D5$ is already broken softly at the right-handed neutrino mass scale, one can have tiny mass splitting between the two η_i , ($i = 1, 2$) scalars. Thus the lightest among the two η_i , ($i = 1, 2$) can serve as a dark matter candidate.

We now have the essential components of the model ready in our hands to delineate the left-handed Majorana neutrino mass matrix originating from Fig. (1). The detailed expressions for it will be presented afterwards but for the time being let us have a sketchy idea of how the one-loop diagram [23] in Fig. (1) contributes to the left-handed Majorana mass matrix. At this point, a few simplifying assumptions are required to make the expressions appear less complicated. Let some combination of the three quartic couplings $\lambda_1, \lambda_2, \lambda_3$ in Eq. (7) be commonly represented by λ . Furthermore, we neglect the mass splitting between η_1 and η_2 and assume m_0 to be the common mass of these scalar. Let η_{Rj} be the real part of η_j^0 and η_{Ij} be the imaginary part of η_j^0 . We can take the splitting between the masses of η_{Rj} and η_{Ij} to be proportional to λv_j which can be generally a small quantity.

Once again, it is crucial to remind ourselves that ν_ζ for ($\zeta = \mu, \tau$) transform as 2_1 under $D5$, while the $D5$ charge of ν_e is 1_1 . This will play an important role in determining the structure of the left-handed Majorana neutrino mass matrix via the Yukawa couplings given in Eq. (8) at the two Dirac vertices in Fig. (1). Let m_R denote the average mass of the heavy right-handed neutrino states. Hence we can define $z \equiv \frac{m_R^2}{m_0^2}$. In order to define z , we do not distinguish between masses of the two right-handed neutrinos as the quantity z appears only in the logarithm throughout the analysis. Now we can write the second diagonal entry of $M_{\nu L}^{flavour}$ as:

$$(M_{\nu L}^{flavour})_{22}|_{(\text{Model 1})} = \lambda \frac{v_m v_n}{8\pi^2} \frac{y_2^2}{m_{R22}} [\ln z - 1]. \quad (12)$$

This expression in Eq. (12) is valid in limit $m_R^2 \gg m_0^2$. From Eq. (8), it is clear to us that ν_μ

couples to N_{2R} only with Yukawa coupling y_2 . Therefore for $(M_{\nu_L}^{flavour})_{22}$, ν_μ couples to N_{2R} at both the Dirac vertices. Thus $(M_{\nu_L}^{flavour})_{22}$ receives contributions only from m_{R22} with y_2 being the only Yukawa coupling appearing in it. One can obtain the expression for $(M_{\nu_L}^{flavour})_{33}$ in an exactly similar way just by replacing m_{R22} by m_{R11} in Eq. (12).

Moving on to the off-diagonal (2,3) entry of $M_{\nu_L}^{flavour}$ viz. $(M_{\nu_L}^{flavour})_{23}$. Here ν_μ contributes at one of the Dirac vertices while ν_τ contributes at the other one. As we know from Eq. (8), ν_μ and ν_τ couple with N_{2R} and N_{1R} respectively leading to existence of N_{2R} at one of the Dirac vertices and N_{1R} at the other one. Thus $(M_{\nu_L}^{flavour})_{23}$ will receive contributions from off-diagonal entries m_{R12} of the right-handed neutrino mass matrix M_{ν_R} shown in Eq. (11) together with diagonal entries m_{R11} and m_{R22} . It is noteworthy, that the Yukawa coupling appearing at both the Dirac vertices is y_2 as can be seen from Eq. (8). Therefore we get:

$$(M_{\nu_L}^{flavour})_{23}|_{(\text{Model 1})} = \lambda \frac{v_m v_n}{8\pi^2} \frac{y_2^2 m_{R12}}{m_{R11} m_{R22}} [\ln z - 1]. \quad (13)$$

We have used mass insertion approximation while obtaining Eq. (13). The same procedure can be followed to obtain the expressions for the (1,1), (1,2) and (1,3) entries of the left-handed Majorana neutrino mass matrix $M_{\nu_L}^{flavour}$.

In order to make the expressions for the elements of $M_{\nu_L}^{flavour}$ look less cumbersome, we absorb everything else in RHS of Eqs. (12) and (13) except the quartic couplings, Yukawa couplings and the vevs in some loop contributing factors denoted by $r_{\alpha\beta}$ as shown below:

$$\begin{aligned} r_{11} &\equiv \frac{1}{8\pi^2 m_{R11}} [\ln z - 1], \\ r_{22} &\equiv \frac{1}{8\pi^2 m_{R22}} [\ln z - 1], \\ r_{12} &\equiv \frac{m_{R12}}{8\pi^2 m_{R11} m_{R22}} [\ln z - 1]. \end{aligned} \quad (14)$$

Using Eqs. (12), (13), (14) and (7), the left-handed Majorana neutrino mass matrix produced radiatively with Fig. (1) at one-loop level is given by:

$$M_{\nu_L}^{flavour}|_{(\text{Model 1})} = \begin{pmatrix} \chi_1 & \chi_4 & \chi_5 \\ \chi_4 & \chi_2 & \chi_6 \\ \chi_5 & \chi_6 & \chi_3 \end{pmatrix}. \quad (15)$$

Here,

$$\begin{aligned} \chi_1 &\equiv y_1^2 [4r_{12}v_1v_2(\lambda_3 + \lambda_1 - \lambda_2) + (r_{11}v_1^2 + r_{22}v_2^2)(\lambda_1 + \lambda_2)] \\ \chi_2 &\equiv y_2^2 [r_{22}(\lambda_1 + \lambda_2)v_1^2] \\ \chi_3 &\equiv y_2^2 [r_{11}(\lambda_1 + \lambda_2)v_2^2] \\ \chi_4 &\equiv y_1y_2 [r_{12}(\lambda_1 + \lambda_2)v_1^2 + 2r_{22}(\lambda_3 + \lambda_1 - \lambda_2)v_1v_2] \\ \chi_5 &\equiv y_1y_2 [r_{12}(\lambda_1 + \lambda_2)v_2^2 + 2r_{11}(\lambda_3 + \lambda_1 - \lambda_2)v_1v_2] \\ \chi_6 &\equiv y_2^2 [2r_{12}(\lambda_3 + \lambda_1 - \lambda_2)v_1v_2]. \end{aligned} \quad (16)$$

Needless to mention that $\langle \Phi_j \rangle \equiv v_j$ with $(j = 1, 2)$ in Eq. (16).

As already mentioned in Section (I), we will at first try to obtain the form of the left-handed Majorana neutrino mass matrix in Eq. (4) characterized by $\theta_{13} = 0$, $\theta_{23} = \pi/4$ and θ_{12}^0 corresponding to any of the popular mixing values given in Table (1). For this we need $\chi_1 \neq \chi_2 = \chi_3$ together with $\chi_4 = \chi_5$. As we can see from Eq. (16), one can get this by setting $v_1 = v_2 = v$ and $r_{11} = r_{22} = r$. In the right-handed neutrino mass matrix in Eq. (11), the condition $r_{11} = r_{22} = r$ will manifest as:

$$M_{\nu_R} = \frac{1}{2} \begin{pmatrix} m_{R_{11}} & m_{R_{12}} \\ m_{R_{12}} & m_{R_{11}} \end{pmatrix}. \quad (17)$$

We have used Eq. (14) to calculate Eq. (17). A glance at Eq. (17) will immediately reveal that the $r_{11} = r_{22} = r$ criterion basically means maximal mixing between the two right-handed neutrino states N_{1R} and N_{2R} as we discussed earlier in Section (I). Summing up, in order to get the structure of $M_{\nu_L}^{flavour}$ as in Eq. (4) in Model 1, one has to make $v_1 = v_2 = v$ and mixing between N_{1R} and N_{2R} maximal i.e., $r_{11} = r_{22} = r$. Applying these conditions in the general form of $M_{\nu_L}^{flavour}$ for Model 1 given in Eq. (15) one can get:

$$M_{\nu_L}^{flavour}|_{(\text{Model 1})} = v^2 \begin{pmatrix} y_1^2[4r_{12}\lambda_{123} + 2r\lambda_{12}] & y_1y_2[r_{12}\lambda_{12} + 2r\lambda_{123}] & y_1y_2[r_{12}\lambda_{12} + 2r\lambda_{123}] \\ y_1y_2[r_{12}\lambda_{12} + 2r\lambda_{123}] & y_2^2r\lambda_{12} & y_2^2(2r_{12}\lambda_{123}) \\ y_1y_2[r_{12}\lambda_{12} + 2r\lambda_{123}] & y_2^2(2r_{12}\lambda_{123}) & y_2^2r\lambda_{12} \end{pmatrix}. \quad (18)$$

In Eq. (18) we have introduced the compact notation: $\lambda_{12} \equiv \lambda_1 + \lambda_2$ and $\lambda_{123} \equiv \lambda_3 + \lambda_1 - \lambda_2$. To achieve the form of $M_{\nu_L}^{flavour}$ mentioned in Eq. (4) from Eq. (18) within the framework of Model 1 one has to do the following mappings:

$$\begin{aligned} a &\equiv y_1^2v^2[4r_{12}\lambda_{123} + 2r\lambda_{12}] = y_1^2v^2[4r_{12}(\lambda_3 + \lambda_1 - \lambda_2) + 2r(\lambda_1 + \lambda_2)] \\ b &\equiv y_2^2v^2r\lambda_{12} = y_2^2v^2r(\lambda_1 + \lambda_2) \\ c &\equiv y_1y_2v^2[r_{12}\lambda_{12} + 2r\lambda_{123}] = y_1y_2v^2[r_{12}(\lambda_1 + \lambda_2) + 2r(\lambda_3 + \lambda_1 - \lambda_2)] \\ d &\equiv y_2^2v^2(2r_{12}\lambda_{123}) = y_2^2v^2[2r_{12}(\lambda_3 + \lambda_1 - \lambda_2)]. \end{aligned} \quad (19)$$

This brings us to the completion of our first task, i.e., generating the form of the left-handed Majorana neutrino mass matrix in Eq. (4) corresponding to $\theta_{13} = 0$, $\theta_{23} = \pi/4$ and θ_{12}^0 of any of the popular lepton mixing values.

Next, our job is to achieve realistic neutrino mixing i.e., non-zero θ_{13} , deviation of θ_{23} from $\pi/4$ and small modification of the solar mixing angle θ_{12}^0 in our model. For this to happen, we will have to tinker the maximal mixing between the two right-handed neutrino states by a small amount or in other words we will have to shift from the choice of $r_{11} = r_{22} = r$ and allow the two diagonal entries of the right-handed Majorana neutrino mass matrix to differ from each other by a little amount. Thus we now set $r_{22} = r_{11} + \epsilon$, where ϵ is a small quantity. Therefore we are now again back to the most general scenario of M_{ν_R} exhibiting non-maximal mixing between the two right-handed neutrino states N_{1R} and N_{2R} as shown in Eq. (11). Keeping $v_1 = v_2 = v$ condition unchanged and allowing a little shift from maximal mixing between N_{1R} and N_{2R} i.e., applying $r_{22} = r_{11} + \epsilon$, we can get the left-handed Majorana neutrino mass matrix that can be dissociated into two parts viz. a dominant part M^0 that appears similar to the $M_{\nu_L}^{flavour}$ in Eq. (18) and a sub-dominant contribution given by M' which in its turn is proportional to the tiny shift ϵ :

$$M_{\nu_L}^{flavour} = M^0 + M'. \quad (20)$$

Here⁹,

$$M^0|_{(\text{Model 1})} = v^2 \begin{pmatrix} y_1^2[4r_{12}\lambda_{123} + 2r_{11}\lambda_{12}] & y_1y_2[r_{12}\lambda_{12} + 2r_{11}\lambda_{123}] & y_1y_2[r_{12}\lambda_{12} + 2r_{11}\lambda_{123}] \\ y_1y_2[r_{12}\lambda_{12} + 2r_{11}\lambda_{123}] & y_2^2r_{11}\lambda_{12} & y_2^2(2r_{12}\lambda_{123}) \\ y_1y_2[r_{12}\lambda_{12} + 2r_{11}\lambda_{123}] & y_2^2(2r_{12}\lambda_{123}) & y_2^2r_{11}\lambda_{12} \end{pmatrix}, \quad (21)$$

and

$$M'|_{(\text{Model 1})} = \epsilon \begin{pmatrix} x & y & 0 \\ y & x' & 0 \\ 0 & 0 & 0 \end{pmatrix}. \quad (22)$$

The x , y and x' in Eq. (22) are given by:

$$\begin{aligned} x &\equiv y_1^2v^2\lambda_{12} = y_1^2v^2(\lambda_1 + \lambda_2) \\ x' &\equiv y_2^2v^2\lambda_{12} = y_2^2v^2(\lambda_1 + \lambda_2) \\ y &\equiv 2y_1y_2v^2\lambda_{123} = 2y_1y_2v^2(\lambda_3 + \lambda_1 - \lambda_2). \end{aligned} \quad (23)$$

It is straightforward to note that M^0 in Eq. (21) has the same form as that of the left-handed Majorana neutrino mass matrix with $\theta_{13} = 0$, $\theta_{23} = \pi/4$ and θ_{12}^0 of any of the popular mixing choices as shown in Eq. (4) if we identify:

$$\begin{aligned} a' &\equiv y_1^2v^2[4r_{12}\lambda_{123} + 2r_{11}\lambda_{12}] = y_1^2v^2[4r_{12}(\lambda_3 + \lambda_1 - \lambda_2) + 2r_{11}(\lambda_1 + \lambda_2)] \\ b' &\equiv y_2^2v^2r_{11}\lambda_{12} = y_2^2v^2r_{11}(\lambda_1 + \lambda_2) \\ c' &\equiv y_1y_2v^2[r_{12}\lambda_{12} + 2r_{11}\lambda_{123}] = y_1y_2v^2[r_{12}(\lambda_1 + \lambda_2) + 2r_{11}(\lambda_3 + \lambda_1 - \lambda_2)] \\ d' &\equiv y_2^2v^2(2r_{12}\lambda_{123}) = y_2^2v^2[2r_{12}(\lambda_3 + \lambda_1 - \lambda_2)] \end{aligned} \quad (24)$$

just as we did¹⁰ for Eq. (19).

One can employ non-degenerate perturbation theory calculation techniques to obtain the corrections offered to the eigenvalues and eigenvectors of M^0 by M' . Needless to mention that the columns of the U^0 mixing matrix in Eq. (2) represents the unperturbed flavour basis. For the equations to look less complicated we define:

$$\gamma \equiv (b' - 3d' - a') \quad \text{and} \quad \rho \equiv \sqrt{a'^2 + b'^2 + 8c'^2 + d'^2 - 2a'b' - 2a'd' + 2b'd'}. \quad (25)$$

The third ket after including first-order corrections looks like:

$$|\psi_3\rangle|_{(\text{Model 1})} = \begin{pmatrix} \frac{\epsilon}{\gamma^2 - \rho^2} [\rho(\sqrt{2}y \cos 2\theta_{12}^0 - x' \sin 2\theta_{12}^0) - \gamma\sqrt{2}y] \\ -\frac{1}{\sqrt{2}}[1 + \xi\epsilon] \\ \frac{1}{\sqrt{2}}[1 - \xi\epsilon] \end{pmatrix}. \quad (26)$$

The ξ in Eq. (26) is given by:

$$\xi \equiv [\gamma x' + \rho(x' \cos 2\theta_{12}^0 + \sqrt{2}y \sin 2\theta_{12}^0)]/(\gamma^2 - \rho^2). \quad (27)$$

In a CP-conserving situation:

$$\sin \theta_{13} = \frac{\epsilon}{\rho^2 - \gamma^2} [\rho(\sqrt{2}y \cos 2\theta_{12}^0 - x' \sin 2\theta_{12}^0) - \gamma\sqrt{2}y]. \quad (28)$$

⁹We will see in Section (II.2), the M^0 for both Model 1 and Model 2 have the same basic structure although the M' for the two models appear to be different.

¹⁰To distinctly identify the $r_{11} = r_{22} = r$ scenario from the $r_{22} = r_{11} + \epsilon$ case, a primed notation has been used here.

Thus one can easily get non-zero θ_{13} in terms of the model parameters such as ϵ , the vev of the scalars v and the quartic couplings λ_i , ($i = 1, 2, 3$) using Eqs. (24), (25) and (28).

Eq. (26) can also yield an expression for the deviation of θ_{23} from $\pi/4$:

$$\tan \varphi \equiv \tan(\theta_{23} - \pi/4) = \xi \epsilon. \quad (29)$$

From the first-order corrections to the first and the second ket, one can easily compute the corrections to the solar mixing angle θ_{12} :

$$\tan \theta_{12} = \frac{\sin \theta_{12}^0 + \epsilon \beta \cos \theta_{12}^0}{\cos \theta_{12}^0 - \epsilon \beta \sin \theta_{12}^0}, \quad (30)$$

with

$$\beta \equiv \frac{\left[\frac{y}{\sqrt{2}} \cos 2\theta_{12}^0 + \frac{1}{2}(x - \frac{x'}{2}) \sin 2\theta_{12}^0 \right]}{\rho}. \quad (31)$$

It is obvious from Eqs. (30) and (29), that one can obtain the modified θ_{12} and θ_{23} deviation from $\pi/4$ respectively in terms of the parameters of Model 1 with the help of Eqs. (24), (25), (27) and (31).

In this whole discussion of Model 1, we have limited ourselves to the CP-conserving scenario by keeping $r_{\alpha\beta}$, ($\alpha, \beta = 1, 2$) real. One can of course, in general have complex $r_{\alpha\beta}$ by assigning Majorana phases to the right-handed neutrino masses. In such a situation, ϵ will become complex that can produce CP-violation from Eq. (26).

Before closing our discussion on Model 1, let us discuss the prospects of flavour changing decays of charged leptons in this model. As expected, the charged lepton flavour violation (LFV) is governed by the Yukawa Lagrangian analogous to that given in Eq. (8):

$$\mathcal{L}_{\text{LFV}}|_{(\text{Model 1})} = y_1 [(\bar{N}_{2R}\eta_2^+ + \bar{N}_{1R}\eta_1^+)e^-] + y_2 [(\bar{N}_{1R}\eta_2^+)\tau^- + (\bar{N}_{2R}\eta_1^+)\mu^-] + h.c. \quad (32)$$

The LFV processes at one-loop level in Model 1 can occur through diagram¹¹ as shown in Fig. (2). It is evident from Eq. (32), that the kinematically allowed processes like $\mu^- \rightarrow e^- \gamma$, $\tau^- \rightarrow e^- \gamma$ and $\tau^- \rightarrow \mu^- \gamma$ through Fig. (2) is forbidden by the symmetries in the model. This is precisely due to the fact that Eq. (32) prohibits the combination of the η_i and N_α required at the two Yukawa vertices of Fig. (2) to mediate LFV processes. Therefore the LFV processes at one-loop level are strictly forbidden by D_5 symmetry in this model. We now conclude our analysis of Model 1 here. In the following section we will explore Model 2.

II.2 Model 2

As stated earlier in Section (I), Model 2 has fields similar to that of Model 1 except for the fact that the D_5 quantum numbers of the fields in Model 2 differ from that in Model 1. For Model 2 also, let us denote the three left-handed lepton $SU(2)_L$ doublets contained in it by $L_{\zeta L} \equiv (\nu_\zeta \ \zeta^-)_L^T$ with $\zeta = e, \mu, \tau$. Out of these, the two left-handed lepton $SU(2)_L$ doublets i.e., $L_{\mu L}$ and $L_{\tau L}$ form a 2_2 of D_5 while we assign the D_5 quantum number 1_1 to L_{eL} . Two right-handed neutrinos, singlet of SM gauge group are also present in Model 2 that constitute a 2_1 of D_5 . In the scalar sector of Model 2 we have two $SU(2)_L$

¹¹We will see in Section (II.2) the same diagram shown in Fig. (2) can also give rise to LFV decays for Model 2 at one-loop level which can be prohibited by D_5 symmetry. Thus Fig. (2) is valid for both Model 1 and Model 2.

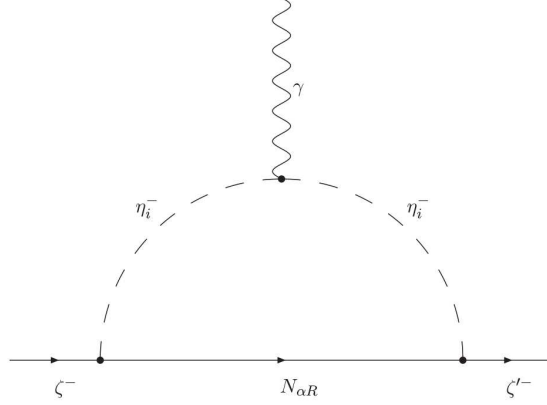


Figure 2: Diagram for charged lepton decay at one-loop for both Model 1 and Model 2. Here ζ^- and ζ'^- represent (e^-, μ^-, τ^-) . In case of charge lepton flavour violating (LFV) decays $\zeta^- \neq \zeta'^-$. Only the processes $\mu^- \rightarrow e^- \gamma$, $\tau^- \rightarrow e^- \gamma$ and $\tau^- \rightarrow \mu^- \gamma$ are kinematically allowed and thus people search for these decays. LFV decays at one-loop level via this diagram are forbidden by $D5$ symmetry in both Model 1 and Model 2.

inert doublet scalars namely, $\eta_i \equiv (\eta_i^+, \eta_i^0)^T$, ($i = 1, 2$) forming a 2_1 of $D5$ given by η . Along with η , the scalar sector is adorned by two $SU(2)_L$ doublet scalars i.e., $\Phi_j \equiv (\phi_j^+, \phi_j^0)^T$, ($j = 1, 2$) having $D5$ quantum number 2_1 denoted by Φ . There is an unbroken Z_2 also present in the model along with $D5$. All the fields except the scalars η and the two right-handed neutrinos are even under this unbroken Z_2 . After SSB, the Z_2 even ϕ_j fields get vev but Z_2 odd η_i scalars do not get any vev. Here also, the vev of ϕ_j^0 is given by v_j i.e., $\langle \Phi_j \rangle \equiv v_j$, ($j = 1, 2$). All the fields in Model 2 with their corresponding quantum numbers are displayed¹² in Table (3). In Model 2 also, we delimit our study to the neutrino sector only. We work in the basis in which charged-lepton mass matrix is diagonal and the whole mixing arises from the neutrino sector.

We follow the same technique used in Model 1 to analyze Model 2. The radiative neutrino mass at one-loop level in Model 2 can be generated by the same diagram as in Model 1 i.e., Fig. (1). From the $D5$ product rules in Appendix (A), it is evident that the total scalar potential as well as the relevant part of it viz. $V_{relevant}$ containing all the $(\eta^\dagger \phi)(\eta^\dagger \phi)$ terms¹³ that regulate the structure of the left-handed Majorana neutrino mass matrix in Model 2 are the same as in Model 1. Therefore the $V_{relevant}$ for Model 2 is given by Eq. (7) mentioned in the previous section¹⁴.

As usual, all symmetries are conserved at all the three vertices we have in Fig. (1). The $D5 \times Z_2$ conserving Dirac vertices can be written as:

$$\mathcal{L}_{Yukawa}|_{(\text{Model 2})} = \tilde{y}_1 [(\overline{N}_{2R}\eta_1^0 + \overline{N}_{1R}\eta_1^0)\nu_e] + \tilde{y}_2 [(\overline{N}_{2R}\eta_1^0)\nu_\tau + (\overline{N}_{1R}\eta_2^0)\nu_\mu] + h.c. \quad (33)$$

¹²A glance at Table (2) and Table (3) will immediately reveal that the fields with $D5$ quantum number 2_2 in Model 1 has been assigned $D5$ charge 2_1 in Model 2 and vice versa. This in fact, is the main difference between Model 1 and Model 2.

¹³Since Fig. (1) is common to both Model 1 and Model 2, two η are created and two ϕ are extirpated at the four-point scalar vertex causing $(\eta^\dagger \phi)(\eta^\dagger \phi)$ terms of the scalar potential to be the one relevant for the analysis in Model 2 also.

¹⁴In other words, in spite of the differences between the $D5$ quantum numbers of the scalars in Model 1 and Model 2, from the product rules in Appendix (A) it can be easily perceived that the scalar potential for Model 1 and Model 2 are exactly identical as discussed in Appendix (B).

Leptons	$SU(2)_L$	$D5$	Z_2
$L_{eL} \equiv (\nu_e \ e^-)_L$	2	1_1	1
$L_{\zeta L} \equiv \begin{pmatrix} \nu_\mu & \mu^- \\ \nu_\tau & \tau^- \end{pmatrix}_L$	2	2_2	1
$N_{\alpha R} \equiv \begin{pmatrix} N_{1R} \\ N_{2R} \end{pmatrix}$	1	2_1	-1
Scalars	$SU(2)_L$	$D5$	Z_2
$\Phi \equiv \begin{pmatrix} \phi_1^+ & \phi_1^0 \\ \phi_2^+ & \phi_2^0 \end{pmatrix}$	2	2_1	1
$\eta \equiv \begin{pmatrix} \eta_1^+ & \eta_1^0 \\ \eta_2^+ & \eta_2^0 \end{pmatrix}$	2	2_1	-1

Table 3: Field content of Model 2 along with their respective charges. Our study here is delimited to the neutrino sector only.

As the D_5 quantum numbers of the left-handed neutrinos ν_ζ for ($\zeta = \mu, \tau$) is 2_2 whereas that of ν_e is 1_1 , we have different Yukawa couplings for them denoted by \tilde{y}_2 and \tilde{y}_1 respectively in Eq. (33). It is also worth pointing out that owing to the difference between the $D5$ charges of the fields in Model 1 and Model 2, we assign different names to the Yukawa couplings of Model 2 in Eq. (33) i.e., \tilde{y}_i , ($i = 1, 2$) compared to the Yukawa couplings of Model 1 given by y_i , ($i = 1, 2$) in Eq. (8). It must also be noted that the \tilde{y}_2 term in Eq. (33) of Model 2 looks substantially different from the y_2 term Eq. (8) of Model 1 because of the difference between $D5$ charges of the fields in Model 1 and Model 2.

In the right-handed neutrino sector of Model 2, essentially one can follow the same steps as in Model 1 to achieve the right-handed Majorana neutrino mass matrix as in Eq. (11). Although the $D5$ charge of the right-handed neutrino fields is 2_1 in Model 2 whereas it is 2_2 in Model 1, from the product rules in Appendix (A), it is easy to comprehend that one can achieve exactly the same direct mass term as in Eq. (9), allow the same soft $D5$ breaking terms as in Eq. (10) and finally obtain the same right-handed neutrino mass matrix $M_{\nu R}$ as in Eq. (11) for Model 2 as well.

As there is no difference in the essential inputs required to tackle the dark matter part as well as the Z_2 charges of the fields in Model 1 and Model 2, we can handle the dark matter sector of Model 2 exactly in the same way¹⁵ as we did in Model 1 and identify the lightest of the η_i , ($i = 1, 2$) fields to be the

¹⁵Since one can replicate the same assumptions and steps in Model 2 in analogy to Model 1, we are not repeating the discussion about the dark matter candidate here again. One can refer to the relevant part of Section (II.1) to explore it in more details.

dark matter component of Model 2 as we did for Model 1.

The next step in the procedure is to discuss the contributions coming from the one-loop diagram in Fig. (1) to the left-handed Majorana neutrino mass matrix in Model 2. For this purpose, we follow similar logical steps and make similar assumptions one by one as we did in Section (II.1) for Model 1 with necessary alterations required for Model 2 taken into account¹⁶. In the similar fashion we can define $z \equiv \frac{m_R^2}{m_0^2}$ and write down the second diagonal entry of $M_{\nu_L}^{flavour}$ in the limit $m_R^2 \gg m_0^2$ as¹⁷:

$$(M_{\nu_L}^{flavour})_{22}|_{(\text{Model 2})} = \lambda \frac{v_m v_n}{8\pi^2} \frac{(\tilde{y}_2)^2}{m_{R_{11}}} [\ln z - 1]. \quad (34)$$

Note that the RHS of Eq. (34) contains $m_{R_{11}}$ whereas the RHS of Eq. (12) has $m_{R_{22}}$. This is primarily due to the difference between the \tilde{y}_2 term of Eq. (33) and y_2 term of Eq. (8) which is the manifestation of the differences between the $D5$ quantum numbers of the fields in Model 2 and Model 1. Keeping in mind the essential features of the \tilde{y}_2 term of Eq. (33), one can obtain the expression for $(M_{\nu_L}^{flavour})_{33}$ for Model 2 by simply replacing $m_{R_{11}}$ of Eq. (34) by $m_{R_{22}}$, in an analogous manner as we did for Model 1 in Section (II.1).

Applying similar logic as for Eq. (13) of Model 1 in Section (II.1) and using the \tilde{y}_2 term of Eq. (33) together with the mass insertion approximation, we can calculate the off-diagonal entry $(M_{\nu_L}^{flavour})_{23}$ for Model 2 also:

$$(M_{\nu_L}^{flavour})_{23}|_{(\text{Model 2})} = \lambda \frac{v_m v_n}{8\pi^2} \frac{(\tilde{y}_2)^2 m_{R_{12}}}{m_{R_{11}} m_{R_{22}}} [\ln z - 1]. \quad (35)$$

Expressions for the rest of the entries of $M_{\nu_L}^{flavour}$ such as the (1,1), (1,2) and (1,3) elements can be deduced in a similar way.

We can absorb all the entities in the RHS of Eqs. (34) and (35) except λ , \tilde{y}_i and v_i in some loop-contributing factors just as we did in Eq. (14) of Section (II.1) for Model 1. In fact, we can use the same definitions of $r_{\alpha\beta}$ as in Eq. (14) for Model 2 also.

Utilizing Eqs. (34), (35), (14) and (7) we can write $M_{\nu_L}^{flavour}$ for Model 2 just as we did in Eq. (15) for Model 1 as:

$$M_{\nu_L}^{flavour}|_{(\text{Model 2})} = \begin{pmatrix} \tilde{\chi}_1 & \tilde{\chi}_4 & \tilde{\chi}_5 \\ \tilde{\chi}_4 & \tilde{\chi}_2 & \tilde{\chi}_6 \\ \tilde{\chi}_5 & \tilde{\chi}_6 & \tilde{\chi}_3 \end{pmatrix}. \quad (36)$$

The $\tilde{\chi}_k$ with $(k = 1, 2, 3, \dots, 6)$ in Eq. (36) is given by:

$$\begin{aligned} \tilde{\chi}_1 &\equiv (\tilde{y}_1)^2 [4r_{12}v_1v_2(\lambda_3 + \lambda_1 - \lambda_2) + (r_{11}v_1^2 + r_{22}v_2^2)(\lambda_1 + \lambda_2)] \\ \tilde{\chi}_2 &\equiv (\tilde{y}_2)^2 [r_{11}(\lambda_1 + \lambda_2)v_2^2] \\ \tilde{\chi}_3 &\equiv (\tilde{y}_2)^2 [r_{22}(\lambda_1 + \lambda_2)v_1^2] \\ \tilde{\chi}_4 &\equiv \tilde{y}_1\tilde{y}_2 [r_{12}(\lambda_1 + \lambda_2)v_2^2 + 2r_{11}(\lambda_3 + \lambda_1 - \lambda_2)v_1v_2] \\ \tilde{\chi}_5 &\equiv \tilde{y}_1\tilde{y}_2 [r_{12}(\lambda_1 + \lambda_2)v_1^2 + 2r_{22}(\lambda_3 + \lambda_1 - \lambda_2)v_1v_2] \\ \tilde{\chi}_6 &\equiv (\tilde{y}_2)^2 [2r_{12}(\lambda_3 + \lambda_1 - \lambda_2)v_1v_2], \end{aligned} \quad (37)$$

¹⁶We are not discussing each step and are just writing down the main equations for Model 2 here. One can refer to the particular discussion available in Section (II.1) for Model 1 as and when needed.

¹⁷For complete insight about the factors m_R , m_0 , z , λ and the associated assumptions required to deduce them, refer to respective discussion in Section (II.1) in context of Model 1. The same remains valid for Model 2 also.

where, $\langle \Phi_j \rangle \equiv v_j$ with $(j = 1, 2)$.

To get the form of the left-handed Majorana neutrino mass matrix as in Eq. (4) corresponding to $\theta_{13} = 0$, $\theta_{23} = \pi/4$ and θ_{12}^0 of any of the popular mixing values given in Table (1), we need to have $\tilde{\chi}_1 \neq \tilde{\chi}_2 = \tilde{\chi}_3$ along with $\tilde{\chi}_4 = \tilde{\chi}_5$ in Eq. (36). This can be achieved by setting $v_1 = v_2 = v$ and $r_{11} = r_{22} = r$ in Eq. (37) just in the same way as we did for Model 1 in Section (II.1). The right-handed neutrino mass matrix once again boils down to the exactly same one as shown in Eq. (17) that corresponds to the maximal mixing between the two right-handed neutrinos N_{1R} and N_{2R} as we have applied $r_{11} = r_{22} = r$ condition. Thus the right-handed neutrino mass matrix after application of $r_{11} = r_{22} = r$ condition in Model 2 is same as that in Model 1 and is given by Eq. (17). Implementing the conditions $v_1 = v_2 = v$ and $r_{11} = r_{22} = r$ in Eq. (36) we get:

$$M_{\nu_L}^{flavour}|_{(\text{Model 2})} = v^2 \begin{pmatrix} (\tilde{y}_1)^2[4r_{12}\lambda_{123} + 2r\lambda_{12}] & \tilde{y}_1\tilde{y}_2[r_{12}\lambda_{12} + 2r\lambda_{123}] & \tilde{y}_1\tilde{y}_2[r_{12}\lambda_{12} + 2r\lambda_{123}] \\ \tilde{y}_1\tilde{y}_2[r_{12}\lambda_{12} + 2r\lambda_{123}] & (\tilde{y}_2)^2r\lambda_{12} & (\tilde{y}_2)^2(2r_{12}\lambda_{123}) \\ \tilde{y}_1\tilde{y}_2[r_{12}\lambda_{12} + 2r\lambda_{123}] & (\tilde{y}_2)^2(2r_{12}\lambda_{123}) & (\tilde{y}_2)^2r\lambda_{12} \end{pmatrix}. \quad (38)$$

Recall, $\lambda_{12} \equiv \lambda_1 + \lambda_2$ and $\lambda_{123} \equiv \lambda_3 + \lambda_1 - \lambda_2$. The following mappings are needed to visualize the $M_{\nu_L}^{flavour}$ in Eq. (38) to be of the form as mentioned in Eq. (4):

$$\begin{aligned} a &\equiv (\tilde{y}_1)^2v^2[4r_{12}\lambda_{123} + 2r\lambda_{12}] = (\tilde{y}_1)^2v^2[4r_{12}(\lambda_3 + \lambda_1 - \lambda_2) + 2r(\lambda_1 + \lambda_2)] \\ b &\equiv (\tilde{y}_2)^2v^2r\lambda_{12} = (\tilde{y}_2)^2v^2r(\lambda_1 + \lambda_2) \\ c &\equiv \tilde{y}_1\tilde{y}_2v^2[r_{12}\lambda_{12} + 2r\lambda_{123}] = \tilde{y}_1\tilde{y}_2v^2[r_{12}(\lambda_1 + \lambda_2) + 2r(\lambda_3 + \lambda_1 - \lambda_2)] \\ d &\equiv (\tilde{y}_2)^2v^2(2r_{12}\lambda_{123}) = \tilde{y}_2^2v^2[2r_{12}(\lambda_3 + \lambda_1 - \lambda_2)]. \end{aligned} \quad (39)$$

To get the realistic neutrino mixings, i.e., non-zero θ_{13} , deviation of θ_{23} from $\pi/4$ and tiny modification of the solar mixing angle θ_{12}^0 in Model 2 one requires to shift from maximal mixing between the two right-handed neutrino states by a small amount ϵ i.e., by applying $r_{22} = r_{11} + \epsilon$ with $v_1 = v_2 = v$. As we discussed for Model 1, here also, applying the condition $r_{22} = r_{11} + \epsilon$ basically causes the right-handed neutrino mass matrix to resume its general form with unequal diagonal entries as in Eq. (11). Putting $r_{22} = r_{11} + \epsilon$ in Eq. (38) with $v_1 = v_2 = v$ condition still valid we can write $M_{\nu_L}^{flavour} = M^0 + M'$ as we did for Model 1 in Eq. (20). The M^0 is the dominant contribution and the M' is the subdominant contribution proportional to ϵ that can be expressed as below:

$$M^0|_{(\text{Model 2})} = v^2 \begin{pmatrix} (\tilde{y}_1)^2[4r_{12}\lambda_{123} + 2r_{11}\lambda_{12}] & \tilde{y}_1\tilde{y}_2[r_{12}\lambda_{12} + 2r_{11}\lambda_{123}] & \tilde{y}_1\tilde{y}_2[r_{12}\lambda_{12} + 2r_{11}\lambda_{123}] \\ \tilde{y}_1\tilde{y}_2[r_{12}\lambda_{12} + 2r_{11}\lambda_{123}] & (\tilde{y}_2)^2r_{11}\lambda_{12} & (\tilde{y}_2)^2(2r_{12}\lambda_{123}) \\ \tilde{y}_1\tilde{y}_2[r_{12}\lambda_{12} + 2r_{11}\lambda_{123}] & (\tilde{y}_2)^2(2r_{12}\lambda_{123}) & (\tilde{y}_2)^2r_{11}\lambda_{12} \end{pmatrix}, \quad (40)$$

and

$$M'|_{(\text{Model 2})} = \epsilon \begin{pmatrix} \tilde{x} & 0 & \tilde{y} \\ 0 & 0 & 0 \\ \tilde{y} & 0 & \tilde{x}' \end{pmatrix}. \quad (41)$$

The \tilde{x} , \tilde{y} and \tilde{x}' mentioned in Eq. (22) can be written as:

$$\begin{aligned} \tilde{x} &\equiv (\tilde{y}_1)^2v^2\lambda_{12} = (\tilde{y}_1)^2v^2(\lambda_1 + \lambda_2) \\ \tilde{x}' &\equiv (\tilde{y}_2)^2v^2\lambda_{12} = (\tilde{y}_2)^2v^2(\lambda_1 + \lambda_2) \\ \tilde{y} &\equiv 2\tilde{y}_1\tilde{y}_2v^2\lambda_{123} = 2\tilde{y}_1\tilde{y}_2v^2(\lambda_3 + \lambda_1 - \lambda_2). \end{aligned} \quad (42)$$

In order to ascertain that the M^0 in Eq. (40) basically has the same form as that of the left-handed Majorana neutrino mass matrix specific to $\theta_{13} = 0$, $\theta_{23} = \pi/4$ and θ_{12}^0 of the popular mixing kind as shown in Eq. (4), one has to make the following identifications¹⁸:

$$\begin{aligned}\tilde{a}' &\equiv (\tilde{y}_1)^2 v^2 [4r_{12}\lambda_{123} + 2r_{11}\lambda_{12}] = (\tilde{y}_1)^2 v^2 [4r_{12}(\lambda_3 + \lambda_1 - \lambda_2) + 2r_{11}(\lambda_1 + \lambda_2)] \\ \tilde{b}' &\equiv (\tilde{y}_2)^2 v^2 r_{11}\lambda_{12} = (\tilde{y}_2)^2 v^2 r_{11}(\lambda_1 + \lambda_2) \\ \tilde{c}' &\equiv \tilde{y}_1\tilde{y}_2 v^2 [r_{12}\lambda_{12} + 2r_{11}\lambda_{123}] = \tilde{y}_1\tilde{y}_2 v^2 [r_{12}(\lambda_1 + \lambda_2) + 2r_{11}(\lambda_3 + \lambda_1 - \lambda_2)] \\ \tilde{d}' &\equiv (\tilde{y}_2)^2 v^2 (2r_{12}\lambda_{123}) = (\tilde{y}_2)^2 v^2 [2r_{12}(\lambda_3 + \lambda_1 - \lambda_2)]\end{aligned}\quad (43)$$

Now we apply non-degenerate perturbation theory to calculate the corrections to M^0 coming from M' . Once again, we remind ourselves that the columns of the U^0 mixing matrix in Eq. (2) are the unperturbed flavour basis. The third ket after getting first order corrections is given by:

$$|\psi_3\rangle_{(\text{Model 2})} = \begin{pmatrix} -\frac{\epsilon}{\tilde{\gamma}^2 - \tilde{\rho}^2} [\tilde{\rho}(\sqrt{2}\tilde{y} \cos 2\theta_{12}^0 - \tilde{x}' \sin 2\theta_{12}^0) - \tilde{\gamma}\sqrt{2}\tilde{y}] \\ -\frac{1}{\sqrt{2}}[1 - \tilde{\xi}\epsilon] \\ \frac{1}{\sqrt{2}}[1 + \tilde{\xi}\epsilon] \end{pmatrix}. \quad (44)$$

where,

$$\tilde{\gamma} \equiv (\tilde{b}' - 3\tilde{d}' - \tilde{a}') \quad \text{and} \quad \tilde{\rho} \equiv \sqrt{\tilde{a}'^2 + \tilde{b}'^2 + 8\tilde{c}'^2 + \tilde{d}'^2 - 2\tilde{a}'\tilde{b}' - 2\tilde{a}'\tilde{d}' + 2\tilde{b}'\tilde{d}'}, \quad (45)$$

and

$$\tilde{\xi} \equiv [\tilde{\gamma}\tilde{x}' + \tilde{\rho}(\tilde{x}' \cos 2\theta_{12}^0 + \sqrt{2}\tilde{y} \sin 2\theta_{12}^0)]/(\tilde{\gamma}^2 - \tilde{\rho}^2). \quad (46)$$

For a CP-conserving situation:

$$\sin \theta_{13} = -\frac{\epsilon}{\tilde{\rho}^2 - \tilde{\gamma}^2} [\tilde{\rho}(\sqrt{2}\tilde{y} \cos 2\theta_{12}^0 - \tilde{x}' \sin 2\theta_{12}^0) - \tilde{\gamma}\sqrt{2}\tilde{y}]. \quad (47)$$

It is straightforward to obtain the non-zero θ_{13} in terms of Model 2 parameters such as ϵ , the vev of the scalars v and λ_i ($i = 1, 2, 3$) using Eqs. (43), (45) and (47). Note the difference in the non-zero θ_{13} yielded by Model 1 in Eq. (28) and that from Model 2 in Eq. (47).

The deviation of θ_{23} from $\pi/4$ can also be calculated from Eq. (47):

$$-\tan \tilde{\varphi} \equiv \tan(\theta_{23} - \pi/4) = -\tilde{\xi}\epsilon. \quad (48)$$

The shift of θ_{23} from $\pi/4$ given by Model 2 in Eq. (48) is different from that given by Model 1 in Eq. (29).

The modifications of θ_{12} can be obtained from the second ket and first ket after including first-order corrections into them as:

$$\tan \theta_{12} = \frac{\sin \theta_{12}^0 + \epsilon\tilde{\beta} \cos \theta_{12}^0}{\cos \theta_{12}^0 - \epsilon\tilde{\beta} \sin \theta_{12}^0}. \quad (49)$$

The $\tilde{\beta}$ in Eq. (49) is given by:

$$\tilde{\beta} \equiv \frac{\left[\frac{\tilde{y}}{\sqrt{2}} \cos 2\theta_{12}^0 + \frac{1}{2}(\tilde{x} - \frac{\tilde{x}'}{2}) \sin 2\theta_{12}^0 \right]}{\tilde{\rho}}. \quad (50)$$

¹⁸We applied the same procedure for Model 1 while obtaining Eq. (24).

Although the solar mixing in Eq. (30) coming from Model 1 looks very similar to that given by Model 2 in Eq. (49), the main difference lies in the fact that altogether β of Model 1 in Eq. (31) is different from $\tilde{\beta}$ of Model 2 in Eq. (50).

It is trivial to express the corrected solar mixing in Eq. (49) and deviation of atmospheric mixing θ_{23} from $\pi/4$ in Eq. (48) in terms of parameters of Model 2 with help of Eqs. (43), (45), (46) and (50).

A CP-conserving scenario has been studied through-out by keeping $r_{\alpha\beta}$, ($\alpha, \beta = 1, 2$) real. If one considers complex $r_{\alpha\beta}$ by assigning Majorana phases to right-handed neutrinos, then ϵ will develop a complex nature which can give rise to CP-violation from Eq. (44).

In an exactly similar fashion as in Model 1, we can show that LFV at one-loop level is forbidden by $D5$ symmetry in Model 2 also. The Yukawa Lagrangian responsible for charged lepton flavour violation in Model 2:

$$\mathcal{L}_{\text{LFV}}|_{(\text{Model 2})} = \tilde{y}_1 [(\overline{N}_{2R}\eta_2^+ + \overline{N}_{1R}\eta_1^+)e^-] + \tilde{y}_2 [(\overline{N}_{2R}\eta_1^+)\tau^- + (\overline{N}_{1R}\eta_2^+)\mu^-] + h.c. \quad (51)$$

The one-loop diagram for LFV decays viz. Fig. (2) shown in Section (II.1) is valid for Model 2 also. As already discussed in Section (II.1), kinematically allowed LFV decays such as $\mu^- \rightarrow e^- \gamma$, $\tau^- \rightarrow e^- \gamma$ and $\tau^- \rightarrow \mu^- \gamma$ at one-loop level in Model 2 cannot take place through Fig. (2) as the combinations of η_i and N_α needed at the two Yukawa vertices of Fig. (2) for these LFV processes are forbidden by Eq. (51). Thus both in Model 1 and in Model 2, LFV decays at one-loop are prohibited by the $D5$ symmetry.

III Conclusions

In this paper, we have devised a mechanism of scotogenic generation of realistic neutrino mixing at one-loop level with $D5 \times Z_2$ symmetry. We demonstrate this mechanism in two set-ups governed by $D5 \times Z_2$ symmetry viz. Model 1 and Model 2. In the two models, similar fields are present with different $D5$ charges. In both models, two right-handed neutrinos N_{1R} and N_{2R} are present that can be maximally mixed to get the form of left-handed Majorana neutrino mass matrix corresponding to $\theta_{13} = 0$, $\theta_{23} = \pi/4$ and any value of θ_{12}^0 particular to the Tribimaximal (TBM), Bimaximal (BM), Golden Ratio (GR) or other mixings. Minute tinkering with the maximal mixing between N_{1R} and N_{2R} can yield realistic mixings such as non-zero θ_{13} , deviation of θ_{23} from $\pi/4$ and small modification of the solar mixing angle θ_{12}^0 in a single stroke for both the models. In both Model 1 and Model 2, two Z_2 odd inert $SU(2)_L$ doublet scalars η_i ($i = 1, 2$) are present. The lightest of these two η_i is a suitable dark matter candidate for both Model 1 and Model 2.

Acknowledgements: I thank Prof. Amitava Raychaudhuri for useful discussions.

A Appendix: The $D5$ group

Here we present a brief summary of the discrete group $D5$. A detailed description can be found in [18, 19] and [24]. The discrete dihedral symmetry $D5$ basically corresponds to the symmetry of a regular pentagon. The generators of $D5$ are \mathcal{X} and \mathcal{Y} . The group is generated by $2\pi/5$ rotation \mathcal{X} and reflection \mathcal{Y} . The generators satisfy the following relations: $\mathcal{X}^5 = I$, $\mathcal{Y}^2 = I$ and $\mathcal{Y}\mathcal{X}\mathcal{Y} = I$. The group

$D5$ has 10 elements and there are four conjugacy classes. $D5$ has four irreducible representations viz. two one-dimensional representations denoted by 1_1 and 1_2 and two two-dimensional representations 2_1 and 2_2 .

The product rules for $D5$ are as follows:

$$\begin{aligned} 1_1(a) \times 1_1(b) &= 1_2(a) \times 1_2(b) = 1_1(ab), \\ 1_1(a) \times 1_2(b) &= 1_2(a) \times 1_1(b) = 1_2(ab), \end{aligned} \quad (\text{A.1})$$

$$\begin{aligned} 1_1(a) \times 2_k \begin{pmatrix} b_1 \\ b_2 \end{pmatrix} &= 2_k \begin{pmatrix} ab_1 \\ ab_2 \end{pmatrix}, \\ 1_2(a) \times 2_k \begin{pmatrix} b_1 \\ b_2 \end{pmatrix} &= 2_k \begin{pmatrix} ab_1 \\ -ab_2 \end{pmatrix}, \quad (k = 1, 2), \end{aligned} \quad (\text{A.2})$$

$$\begin{aligned} 2_1 \begin{pmatrix} a_1 \\ a_2 \end{pmatrix} \times 2_1 \begin{pmatrix} b_1 \\ b_2 \end{pmatrix} &= 1_1(a_1b_2 + a_2b_1) + 1_2(a_1b_2 - a_2b_1) + 2_2 \begin{pmatrix} a_1b_1 \\ a_2b_2 \end{pmatrix}, \\ 2_2 \begin{pmatrix} a_1 \\ a_2 \end{pmatrix} \times 2_2 \begin{pmatrix} b_1 \\ b_2 \end{pmatrix} &= 1_1(a_1b_2 + a_2b_1) + 1_2(a_1b_2 - a_2b_1) + 2_1 \begin{pmatrix} a_2b_2 \\ a_1b_1 \end{pmatrix}, \\ 2_1 \begin{pmatrix} a_1 \\ a_2 \end{pmatrix} \times 2_2 \begin{pmatrix} b_1 \\ b_2 \end{pmatrix} &= 2_1 \begin{pmatrix} a_2b_1 \\ a_1b_2 \end{pmatrix} + 2_2 \begin{pmatrix} a_2b_2 \\ a_1b_1 \end{pmatrix}. \end{aligned} \quad (\text{A.3})$$

These product rules play a crucial role in the models discussed in this paper.

B Appendix: The scalar potentials of both the models:

The scalar sectors of Model 1 and Model 2 are present in Table (2) and Table (3) respectively. For Model 1, we have two $SU(2)_L$ doublet scalars $\Phi_j \equiv (\phi_j^+, \phi_j^0)^T$, ($j = 1, 2$) that transform as 2_2 of $D5$ denoted by Φ having Z_2 charge $+1$. In addition to that, Model 1 also has a couple of inert $SU(2)_L$ doublet scalars η , given by $\eta_i \equiv (\eta_i^+, \eta_i^0)^T$, ($i = 1, 2$) that transform as 2_2 of $D5$ and the Z_2 quantum number of η is -1 .

The picture is slightly different for Model 2. In the scalar sector of Model 2, the two $SU(2)_L$ doublet scalars $\Phi_j \equiv (\phi_j^+, \phi_j^0)^T$, ($j = 1, 2$), represented by Φ , transform as 2_1 of $D5$ with Z_2 charge $+1$ whereas the inert $SU(2)_L$ doublet scalars $\eta_i \equiv (\eta_i^+, \eta_i^0)^T$, ($i = 1, 2$), compactly denoted by η , transform as 2_1 of $D5$. In Model 2 also, η is odd under Z_2 .

For both Model 1 and Model 2 since Φ is even under Z_2 it can get vev after SSB¹⁹ whereas η being Z_2 odd does not get vev.

From the $D5$ product rules mentioned in Appendix (A), one can easily infer that despite of the difference in the $D5$ charges of Φ and η in Model 1 and Model 2, the complete scalar potential containing all terms permitted by the SM gauge symmetry as well as $D5 \times Z_2$ are same in both the models. The total scalar potential inclusive of all terms allowed by the SM gauge symmetry and $D5 \times Z_2$ for both Model

¹⁹As mentioned earlier, the vevs of ϕ_j^0 is given by v_j i.e., $\langle \Phi_j \rangle \equiv v_j$, ($j = 1, 2$).

1 and Model 2:

$$\begin{aligned}
V_{total} = & m_\eta^2 \left(\eta_2^\dagger \eta_2 + \eta_1^\dagger \eta_1 \right) + m_\phi^2 \left(\phi_2^\dagger \phi_2 + \phi_1^\dagger \phi_1 \right) \\
& + \hat{\lambda}_1 \left(\eta_2^\dagger \eta_2 + \eta_1^\dagger \eta_1 \right)^2 + \hat{\lambda}_2 \left(\eta_2^\dagger \eta_2 - \eta_1^\dagger \eta_1 \right)^2 + \hat{\lambda}_3 \left(\phi_2^\dagger \phi_2 + \phi_1^\dagger \phi_1 \right)^2 + \hat{\lambda}_4 \left(\phi_2^\dagger \phi_2 - \phi_1^\dagger \phi_1 \right)^2 \\
& + \hat{\lambda}_5 \left[\left(\eta_2^\dagger \eta_2 + \eta_1^\dagger \eta_1 \right) \left(\phi_2^\dagger \phi_2 + \phi_1^\dagger \phi_1 \right) \right] + \hat{\lambda}_6 \left[\left(\eta_2^\dagger \eta_2 - \eta_1^\dagger \eta_1 \right) \left(\phi_2^\dagger \phi_2 - \phi_1^\dagger \phi_1 \right) \right] \\
& + \hat{\lambda}_7 \left[\left(\phi_1^\dagger \phi_2 \right) \left(\phi_2^\dagger \phi_1 \right) \right] + \hat{\lambda}_8 \left[\left(\eta_1^\dagger \eta_2 \right) \left(\eta_2^\dagger \eta_1 \right) \right] \\
& + \hat{\lambda}_9 \left[\left\{ \left(\phi_1^\dagger \phi_2 \right) \left(\eta_2^\dagger \eta_1 \right) \right\} + \left\{ \left(\phi_2^\dagger \phi_1 \right) \left(\eta_1^\dagger \eta_2 \right) \right\} \right] + V_{relevant}
\end{aligned} \tag{B.1}$$

with,

$$\begin{aligned}
V_{relevant} = & \lambda_1 \left[\left\{ \left(\eta_2^\dagger \phi_2 + \eta_1^\dagger \phi_1 \right)^2 \right\} + h.c. \right] + \lambda_2 \left[\left\{ \left(\eta_2^\dagger \phi_2 - \eta_1^\dagger \phi_1 \right)^2 \right\} + h.c. \right] \\
& + \lambda_3 \left[\left\{ \left(\eta_1^\dagger \phi_2 \right) \left(\eta_2^\dagger \phi_1 \right) + \left(\eta_2^\dagger \phi_1 \right) \left(\eta_1^\dagger \phi_2 \right) \right\} + h.c. \right].
\end{aligned} \tag{B.2}$$

As already discussed earlier, two η scalars are created and two ϕ fields are obliterated at the four-point scalar vertex of Fig. (1). Thus only the $(\eta^\dagger \phi)(\eta^\dagger \phi)$ terms of the scalar potential take part in determining the left-handed Majorana neutrino mass matrix and hence are relevant for our purpose. We accumulate all such $(\eta^\dagger \phi)(\eta^\dagger \phi)$ terms together in Eq. (B.2) and call it $V_{relevant}$. The couplings λ_j ($j = 1, 2, 3$) in Eq. (B.2) were taken to be real throughout.

References

- [1] For the present status of θ_{13} see presentations from Double Chooz, RENO, Daya Bay, and T2K at Neutrino 2016 (<http://neutrino2016.iopconfs.org/programme>).
- [2] I. Esteban, M. C. Gonzalez-Garcia, M. Maltoni, T. Schwetz and A. Zhou, JHEP **09**, 178 (2020) [arXiv:2007.14792 [hep-ph]], NuFIT 5.2 (2022).
- [3] M. C. Gonzalez-Garcia, M. Maltoni, J. Salvado and T. Schwetz, JHEP **1212**, 123 (2012) [arXiv:1209.3023v3 [hep-ph]], NuFIT 3.2 (2018).
- [4] D. V. Forero, M. Tortola and J. W. F. Valle, Phys. Rev. D **86**, 073012 (2012) [arXiv:1205.4018 [hep-ph]].
- [5] B. Brahmachari and A. Raychaudhuri, Phys. Rev. D **86**, 051302 (2012) [arXiv:1204.5619 [hep-ph]]; S. Pramanick and A. Raychaudhuri, Phys. Rev. D **88**, 093009 (2013) [arXiv:1308.1445 [hep-ph]].
- [6] S. Pramanick and A. Raychaudhuri, Phys. Lett. B **746**, 237 (2015) [arXiv:1411.0320 [hep-ph]]; Int. J. Mod. Phys. A **30**, 1530036 (2015) [arXiv:1504.01555 [hep-ph]].
- [7] P. Minkowski, Phys. Lett. B **67**, 421 (1977); M. Gell-Mann, P. Ramond and R. Slansky, in *Supergravity*, p. 315, edited by F. van Nieuwenhuizen and D. Freedman, North Holland, Amsterdam, (1979); T. Yanagida, Proc. of the *Workshop on Unified Theory and the Baryon Number of the Universe*, KEK, Japan, (1979); S.L. Glashow, NATO Sci. Ser. B **59**, 687 (1980); R.N. Mohapatra and G. Senjanović, Phys. Rev. D **23**, 165 (1981); J. Schechter and J. W. F. Valle, Phys. Rev. D **25**, 774 (1982); J. Schechter and J. W. F. Valle, Phys. Rev. D **22**, 2227 (1980).

- [8] F. Vissani, JHEP **9811**, 025 (1998) [hep-ph/9810435]. Models with somewhat similar points of view as those espoused here are E. K. Akhmedov, Phys. Lett. B **467**, 95 (1999) [hep-ph/9909217] and M. Lindner and W. Rodejohann, JHEP **0705**, 089 (2007) [hep-ph/0703171].
- [9] For other recent work after the determination of θ_{13} see S. Antusch, S. F. King, C. Luhn and M. Spinrath, Nucl. Phys. B **856**, 328 (2012) [arXiv:1108.4278 [hep-ph]]; B. Adhikary, A. Ghosal and P. Roy, Int. J. Mod. Phys. A **28**, 1350118 (2013) arXiv:1210.5328 [hep-ph]; D. Aristizabal Sierra, I. de Medeiros Varzielas and E. Houet, Phys. Rev. D **87**, 093009 (2013) [arXiv:1302.6499 [hep-ph]]; R. Dutta, U. Ch, A. K. Giri and N. Sahu, Int. J. Mod. Phys. A **29**, 1450113 (2014) arXiv:1303.3357 [hep-ph]; L. J. Hall and G. G. Ross, JHEP **1311**, 091 (2013) arXiv:1303.6962 [hep-ph]; T. Araki, PTEP **2013**, 103B02 (2013) arXiv:1305.0248 [hep-ph]; A. E. Carcamo Hernandez, I. de Medeiros Varzielas, S. G. Kovalenko, H. Päs and I. Schmidt, Phys. Rev. D **88**, 076014 (2013) [arXiv:1307.6499 [hep-ph]]; M. -C. Chen, J. Huang, K. T. Mahanthappa and A. M. Wijangco, JHEP **1310**, 112 (2013) [arXiv:1307.7711 [hep-ph]]; B. Brahmachari and P. Roy, JHEP **1502**, 135 (2015) [arXiv:1407.5293 [hep-ph]]; P. S. Bhupal Dev, B. Dutta, R. N. Mohapatra and M. Severson, Phys. Rev. D **86**, 035002 (2012) [arXiv:1202.4012 [hep-ph]].
- [10] For a review see, for example, S. F. King and C. Luhn, Rept. Prog. Phys. **76**, 056201 (2013) [arXiv:1301.1340 [hep-ph]].
- [11] S. Pramanick and A. Raychaudhuri, Phys. Rev. D **94**, no. 11, 115028 (2016) [arXiv:1609.06103 [hep-ph]],
- [12] S. Pramanick, Phys. Rev. D **98**, no. 7, 075016 (2018) [arXiv:1711.03510 [hep-ph]].
- [13] S. Pramanick and A. Raychaudhuri, Phys. Rev. D **93**, no. 3, 033007 (2016) [arXiv:1508.02330 [hep-ph]].
- [14] E. Ma, Phys. Lett. B **671**, 366 (2009) [arXiv:0808.1729 [hep-ph]].
- [15] E. Ma and D. Wegman, Phys. Rev. Lett. **107**, 061803 (2011) [arXiv:1106.4269 [hep-ph]]; S. Gupta, A. S. Joshipura and K. M. Patel, Phys. Rev. D **85**, 031903 (2012) [arXiv:1112.6113 [hep-ph]]; G. C. Branco, R. G. Felipe, F. R. Joaquim and H. Serodio, arXiv:1203.2646 [hep-ph]; B. Adhikary, B. Brahmachari, A. Ghosal, E. Ma and M. K. Parida, Phys. Lett. B **638**, 345 (2006) [hep-ph/0603059]; B. Karmakar and A. Sil, Phys. Rev. D **91**, 013004 (2015) [arXiv:1407.5826 [hep-ph]]; E. Ma, Phys. Lett. B **752**, 198 (2016) [arXiv:1510.02501 [hep-ph]]; X. G. He, Y. Y. Keum and R. R. Volkas, JHEP **0604**, 039 (2006) [hep-ph/0601001].
- [16] S. K. Kang and M. Tanimoto, Phys. Rev. D **91**, no. 7, 073010 (2015) [arXiv:1501.07428 [hep-ph]].
- [17] Kang, O. Popov, R. Srivastava, J. W. F. Valle and C. A. Vaquera-Araujo, arXiv:1902.05966 [hep-ph]; N. Rojas, R. Srivastava and J. W. F. Valle, Phys. Lett. B **789**, 132 (2019) [arXiv:1807.11447 [hep-ph]]; M. A. Díaz, N. Rojas, S. Urrutia-Quiroga and J. W. F. Valle, JHEP **1708**, 017 (2017) [arXiv:1612.06569 [hep-ph]]; A. Merle, M. Platscher, N. Rojas, J. W. F. Valle and A. Vicente, JHEP **1607**, 013 (2016) [arXiv:1603.05685 [hep-ph]]; M. Hirsch, R. A. Lineros, S. Morisi, J. Palacios, N. Rojas and J. W. F. Valle, JHEP **1310**, 149 (2013) [arXiv:1307.8134 [hep-ph]]; C. Bonilla, E. Ma, E. Peinado and J. W. F. Valle, Phys. Lett. B **762**, 214 (2016) [arXiv:1607.03931 [hep-ph]].
- [18] E. Ma, Fizika B **14**, 35-40 (2005) [arXiv:hep-ph/0409288 [hep-ph]].

- [19] C. Hagedorn, M. Lindner and F. Plentinger, Phys. Rev. D **74**, 025007 (2006) [arXiv:hep-ph/0604265 [hep-ph]].
- [20] Y. Cai, J. Herrero-García, M. A. Schmidt, A. Vicente and R. R. Volkas, Front. in Phys. **5**, 63 (2017) [arXiv:1706.08524 [hep-ph]]; C. Klein, M. Lindner and S. Ohmer, arXiv:1901.03225 [hep-ph].
- [21] S. Pramanick, Phys. Rev. D **100**, no.3, 035009 (2019) [arXiv:1904.07558 [hep-ph]].
- [22] S. Pramanick, Nucl. Phys. B **963**, 115282 (2021) doi:10.1016/j.nuclphysb.2020.115282 [arXiv:1903.04208 [hep-ph]].
- [23] E. Ma, Phys. Rev. D **73**, 077301 (2006) [hep-ph/0601225].
- [24] H. Ishimori, T. Kobayashi, H. Ohki, Y. Shimizu, H. Okada and M. Tanimoto, Prog. Theor. Phys. Suppl. **183**, 1-163 (2010) [arXiv:1003.3552 [hep-th]].